ELSEVIER

Polymer 41 (2000) 4691–4698

polymer

A small angle X-ray scattering study of pore structure in Tencel® cellulose fibres and the effects of physical treatments

J. Crawshaw, R.E. Cameron*

University of Cambridge, Department of Materials Science and Metallurgy, New Museums Site, Pembroke Street, Cambridge CB2 3QZ, UK

Received 15 April 1999; received in revised form 14 June 1999; accepted 9 July 1999

Abstract

In situ SAXS experiments were performed as water-swollen lyocell (Tencel®) fibres were repeatedly dried at 160°C and re-wet. In all cases, the void size increased and the void volume fraction decreased on drying. The water-swollen fibre apparently consists of a network of small voids between many of the elementary fibrils. As the water is driven out of the fibre, smaller voids collapse leaving dense regions and a few large voids. Consecutive drying cycles affected the pore structure. The wet volume fraction of voids and the void length parallel to the fibre axis decreased with increasing cycle number. The void parameters perpendicular to the fibre axis did not change significantly. Pre-treatment by autoclaving and drying at 160°C resulted in similar changes. The observations are consistent with the hornification mechanism proposed for native cellulose fibres in which the voids are partially or totally 'zipped up' during drying by the formation of additional hydrogen bonds between elementary fibrils and are thus not able to reopen fully on re-wetting [Stone JE, Scallan AM. Technical section of the British Paper and Board Makers' Association, 1996, p. 1; Laivins GV, Scallan AM. Transcript of products of paper making. In: Baker CF, editor. Tenth Fundamental Research Symposium, vol.2. Oxford: Pira International, 1993, p. 1235; Scallan AM. Fibre–water interactions in paper making. 1. Transactions of BPBIF Symposium, Oxford, 1977]. © 2000 Elsevier Science Ltd. All rights reserved.

Keywords: Reconstituted cellulose fibres; SAXS; Hornification

1. Introduction

Tencel fibre is of the lyocell type spun from a solution of cellulose in tertiary amine N-oxide. Such fibres have a degree of crystallinity of the order of 90%, and are composed of elementary fibrils partially separated by elongated voids, which run parallel to the fibre axis. The elementary fibrils consist of cellulose II crystallites, separated in the fibre-axis direction by highly oriented amorphous regions [1,2]. 'Non-swelling clusters' of fibrils may be formed if the bonding between the neighbouring crystallites is strong [3,4].

The nature of the bonding between the elementary fibrils is thought to affect the ability of the fibre to undergo localised separation of fibrous elements at the surface, known as fibrillation [5]. Cellulose fibres suffer fibrillation if subject to abrasion and this can affect the 'hand' of a fabric. The requirements for the fabric dictate whether or not it is a desirable property; for some uses, the fibres are intentionally fibrillated as part of the production process [6]. Control of the susceptibility of the fibres to fibrillation is therefore of some interest.

In a comparative study of modal and lyocell types of regenerated cellulose fibres, Lenz et al. [5] found that lyocell fibres suffer a higher degree of fibrillation than modal. They also contained a lower proportion of non-swelling bundles of elementary fibrils, attributed to a higher degree of orientation facilitating separation of elementary fibrils. Lenz et al. linked these results, postulating that separated elementary fibrils are more susceptible to fibrillation. A treatment, which changes the degree of bonding between fibres, might change the susceptibility to fibrillation.

When native cellulose fibres are dried there is a subsequent reduction in the extent of swelling when the fibres are re-wet [7–9]. The loss of swelling resulting from a drying and re-wetting cycle is termed 'hornification'. Scallan and co-workers have accounted for hornification by a loss in void volume within the fibre on drying, which is not fully recovered to the original wet void volume on re-wetting. Scallan has proposed a mechanism for hornification [8] in which some voids 'zip up' on drying, by the formation of additional hydrogen bonds between the elementary fibrils. Subsequent re-wetting only causes partial 'unzipping'.

Stone and Scallan [10] compared cellulose fibres dried at 25, 105, and 150°C, and found that higher temperature

* Corresponding author.

0032-3861/00/$ - see front matter © 2000 Elsevier Science Ltd. All rights reserved.
PII: S0032-3861(99)00502-9

results in a higher proportion of irreversibly closed voids on re-swelling. A reduction in the median void size indicated that on drying at higher temperature, permanent closure tends to occur among the larger voids. This study was done mainly on woodpulps, but only one rayon sample was used. No loss of void content was found for the rayon sample, although this is the only regenerated cellulose fibre studied and may not be representative.

The existence of hornification in native cellulose pulps, suggests a route for changing the degree of bonding in Tencel fibres. It is likely that the native and regenerated cellulose fibre structures are sufficiently similar to apply the mechanism to regenerated cellulose fibres. In both native and regenerated cellulose fibres, elongated voids are aligned parallel to the fibre axis, and separated by elementary fibrils or groups of elementary fibrils. The dimensions of elementary fibrils are thought to be slightly different in native and regenerated cellulose fibres, but their basic structure is similar in both fibre types.

This paper reports a study of the effects of treatments designed to affect the degree of bonding in the fibres. Time-resolved SAXS is used to follow the microstructural changes, which occur on drying and re-wetting.

2. Experimental

2.1. Materials

Tencel fibres were produced from a solution of cellulose in NMMO, filtered, spun, washed and then dried by Courtaulds Corporate Technology. These fibres will be referred to as 'untreated'. Some untreated fibres were then autoclaved for 1 h at 110°C and 1.1 atm, and then dried at 160°C. These will be referred to as 'pre-treated'.

2.2. X-ray experiments

Experiments were carried out on station 2.1 of the CCLRC synchrotron radiation source at Daresbury. Approximately 1 mm thick bundles of fibres were placed in a brass sample cell with mica windows and treated in situ in the X-ray beam. First, the fibres were swollen in cold distilled water and then dried at approximately 160°C. The sample was heated using a small hot plate pressed against the mica window of the sample cell. Incident X-rays passed through a hole in the hot plate.

SAXS data were recorded during drying using a two-dimensional gas filled proportional detector, binning at 60 s intervals. When no further changes were observed in the SAXS pattern, and the fibres appeared to be dry, hot fibres were re-swollen in cold distilled water and then dried at approximately 160°C once again. The treatment was repeated four times.

2.3. Data analysis

2.3.1. Standard corrections

The two-dimensional, time-resolved SAXS data were corrected for variations in the incident beam intensity by normalising to the signal from an ionisation chamber placed after the sample. Corrections for the non-uniform response of the detector were made by dividing by the response of the uniformly illuminated detector. The electronic 'tac' hole was removed and the image was rotated if necessary. In addition, an empty sample-cell background was subtracted.

2.3.2. Analysis of the pore structure

The SAXS, for both dry and wet Tencel fibres, was elongated along the equator, and after the work of Statton [11,12] will be interpreted as the scattering by long thin voids, with their long axis showing a preferred orientation parallel to the fibre axis. The meridional broadening seen in the wet fibres will be interpreted as increased misorientation of the voids and a reduction in void length occurring on swelling, after the work of Ruland et al. [13,14].

At each point along the equator, the intensity was summed across the whole width of the detector, in the meridional direction, to produce an integrated equatorial intensity. If **q** represents the scattering vector; with the component q_x parallel to the equatorial, q_y parallel to the incident beam, and q_z parallel to the meridian, then the integrated equatorial intensity is given by

$$\tilde{I}(q_x) = \int_{-\infty}^{\infty} I(\mathbf{q})\, \mathrm{d}q_z \tag{1}$$

In all cases, the integrated equatorial intensity was extrapolated at low q_x using the Guinier method. High q_x extrapolation was empirically estimated in the scattering from wet fibre data by fitting a straight line to a plot of $\tilde{I}(q_x)q_x$ as a function of q_x.

This approximate extrapolation was performed since data were not available at sufficiently high q_x to perform an extrapolation according to Porod's law. Dry fibre data were not extrapolated at high q_x because these data reached a background level within the q_x range of the experimental data. Time-resolved SAXS data collected as water swollen fibres were dried, and extrapolated only at low q_x.

The scattering power, or invariant, Q, was calculated, with the extrapolations described, using

$$Q = \int_{0}^{+\infty} \tilde{I}(q_x) q_x \, \mathrm{d}q_x \tag{2}$$

The parameters L_2, R_3, and S_3, which characterise the voids in the plane perpendicular to the fibre axis, were calculated after the method of Shioya and Takaku [15] using

$$L_2 = \frac{2\int_{0}^{\infty} \tilde{I}(q_x)\, \mathrm{d}q_x}{Q} \tag{3}$$

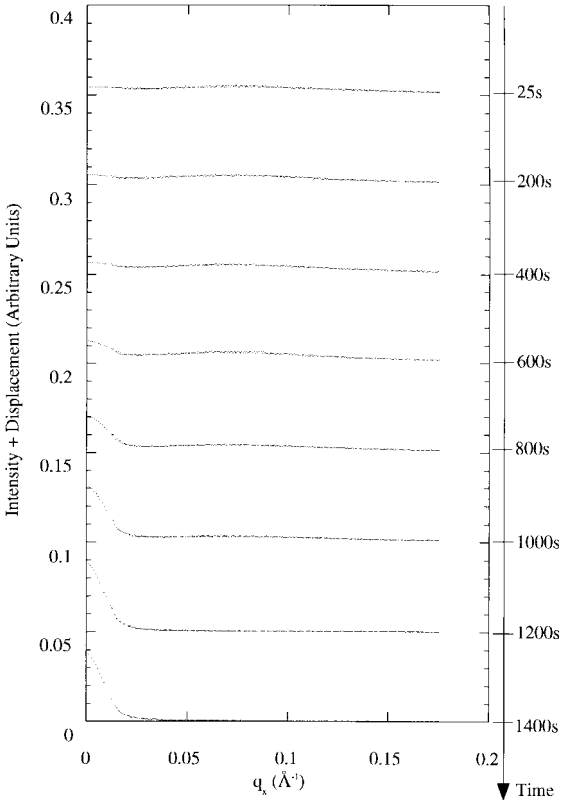

Fig. 1. Time-resolved integrated equatorial SAXS, $\tilde{\imath}(q_x)$, for water-swollen untreated Tencel fibres as they were dried at 160°C. The plot for each individual frame has been off-set by adding a fixed displacement to the intensity.

$$R_3^2 = -2 \operatorname*{Lt}_{q_x \to 0} \frac{\mathrm{d} \ln \tilde{I}(q_x)}{\mathrm{d}q_x^2} \tag{4}$$

and

$$S_3 = \operatorname*{Lt}_{q_x \to 0} \frac{2\pi \tilde{I}(q_x)}{Q} \tag{5}$$

L_2 is the average chord length of a line drawn through the cross-section of the voids at random. R_3 is the average radius of gyration of the cross-section of the voids and S_3 is the mean area of the cross-section of the voids. Void cross-section shape perpendicular to the fibre axis was assessed by treating the cross-sections as rectangles of side X and Y, calculated in terms of R_3 and S_3 using [16]

$$R_3^2 = \frac{X^2 + Y^2}{12} \tag{6}$$

and

$$S_3 = XY \tag{7}$$

If the voids are sufficiently dilute for negligible inter-particle interference, and a two-phase system of cellulose and voids is assumed, then the volume fraction of the voids is given by

$$v \propto \frac{Q}{\rho^2} \tag{8}$$

where ρ is the electron density difference between the voids and cellulose, and Q is the scattering power. Absolute intensities were not available for these SAXS data, therefore the proportionality had to be used to follow changes in the void volume fraction on swelling. When the voids are not dilute the void volume fraction is given by [17]

$$v(1 - v) \propto \frac{Q}{\rho^2} \tag{9}$$

The voids may be assumed to be entirely air filled in dry fibres and entirely water filled in water-swollen fibres. The assumption that no air filled voids remain in water swollen fibres was validated using the SANS contrast variation technique, described elsewhere [18]. The electron density difference ρ between cellulose and voids was calculated to be $\rho \cong 850\mathrm{N_A}$ electrons/m^3 for dry fibres, and $\rho \cong 294\mathrm{N_A}$ electrons/m^3 for wet fibres.

The orientation distribution, B_ϕ, and length projected onto the fibre axis, L_3, of the voids parallel to the fibre axis were estimated from azimuthal scans of the data using the method of Ruland et al. [13,14]. Azimuthal scans were fitted with a Gaussian for estimation of the full-width half maximum, B_{fwhm}. The integral width, B_{obs}, was calculated from B_{fwhm}, using [19]

$$B_{\mathrm{obs}} \cong \frac{B_{\mathrm{fwhm}}}{0.939} \tag{10}$$

Then, $(qB_{\mathrm{obs}})^2$ was plotted as a function of q^2 and a straight line was fitted according to

$$(qB_{\mathrm{obs}})^2 = \frac{(2\pi)^2}{L_3^2} + (qB_\phi)^2 \tag{11}$$

to obtain B_ϕ and L_3.

2.3.3. Limitations of the analysis

Shioya and Takakus' [15] method for analysing SAXS from oriented voids within uniaxially aligned fibres was derived assuming independent particle scattering from dilute packed voids. This is reasonable for dry cellulose fibres. However, closer packing of the voids in water-swollen cellulose fibres gives rise to inter-particle interference. This changes the shape of the SAXS curve, introducing a systematic error in the calculation of the void parameters. Despite the high volume fraction in the wet fibres, the Guinier plots used to calculate R_3 were still fairly straight. This may be a result of a high polydispersity in the void size, which extends the range of validity for the analysis. Because of these problems, trends in changes of the void parameters will be regarded as valid, but magnitudes will be treated with extreme caution.

The data from the wet fibres required extrapolation at high q_x, and an empirical method of convenience was

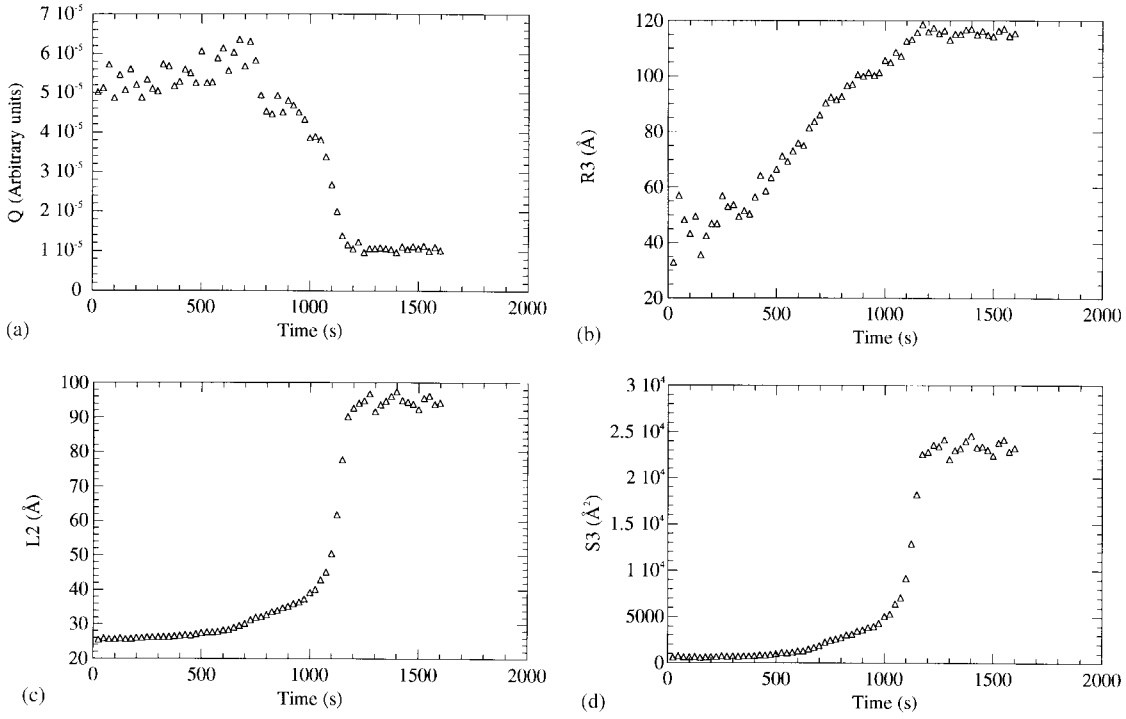

Fig. 2. Changes in the void parameters of water-swollen, previously untreated Tencel fibres as they are dried at 160°C: (a) scattering power Q; (b) mean radius of gyration of the cross-section R_3; (c) mean void cross-section length L_2; and (d) mean void cross-section area S_3.

used. This will introduce inaccuracies in the value of Q and the parameters derived from it. In practice, the parameters obtained were relatively insensitive to this approximation and the trends can be believed. However, it gives yet more reason to treat the magnitudes of the parameters for the wet samples in particular with caution.

Table 1
General trends in changes in the void volume fraction and void cross-section size and shape parameters when untreated water-swollen Tencel fibres were dried at 160°C. An important point to note about the wet fibre values for the rectangular cross section side, X, is that the estimated magnitude is too tiny for scattering into the small angle region. However, as explained in the text, although trends in changes of the void parameters are reliable, magnitudes calculated for the wet fibre void parameters are likely to be inaccurate due to the assumptions made in their calculation

Void parameter	Change in void parameter on drying (water swollen → dry)
Proportional to volume fraction ($Q \times 10^{11} \times N_A^2/\rho^2$)	Decrease ~ (58 → 1) (arbitrary units)
L_2	Increase ~ (25 → 95 Å)
R_3	Increase ~ (45 → 115 Å)
S_3	Increase ~ (500^2 → 22 500 Å^2)
X	Increase ~ (3 → 50 Å)
Y	Increase ~ (110 → 340 Å)
B_ϕ	Decrease ~ (20 → 10°)
L_3	Increase ~ (360 → 2700 Å)

3. Results and discussion

3.1. Pore structure in wet and dry fibres

3.1.1. Observations

Fig. 1 illustrates the time-resolved integrated equatorial SAXS for water-swollen untreated Tencel fibres as it was dried at 160°C: the changes in the profile of the SAXS are typical of all the fibres studied.

Fig. 2 shows the scattering power, Q, the mean void cross-section length, L_2, the mean radius of gyration of the void cross-section, R_3 and the mean void cross section area, S_3, as a function of drying time for the in situ drying of water-swollen untreated Tencel fibres.

Fig. 2(b)–(d) shows that R_3, L_2 and S_3 all increased on drying. Fig. 2(a) shows that Q decreased on drying. This implies an even greater decrease in the volume fraction of voids on drying, when different electron densities are taken into account as in Eqs. (8) and (9).

For a single first drying of water-swollen untreated Tencel fibres, the orientation distribution parameter fell from $B_\phi \cong 20°$ to $B_\phi \cong 10°$ indicating a narrowing of the distribution of void orientation. The void length increased on drying from $L_3 \cong 360$ Å in water-swollen fibres to $L_3 \cong 2700$ Å in dry fibres. Since this figure represents the projection of the void length onto the fibre axis, a small fraction of this increase will be due to the narrowing of the orientation distribution. However, the change in L_3 still represents a large increase in the overall average length of the voids.

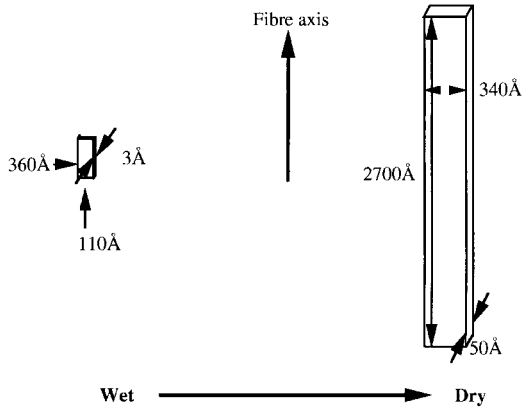

Fig. 3. Schematic representation of changes in the mean void when untreated water-swollen Tencel fibres are dried at 160°C. The void shape has been treated as a rectangular parallelpiped.

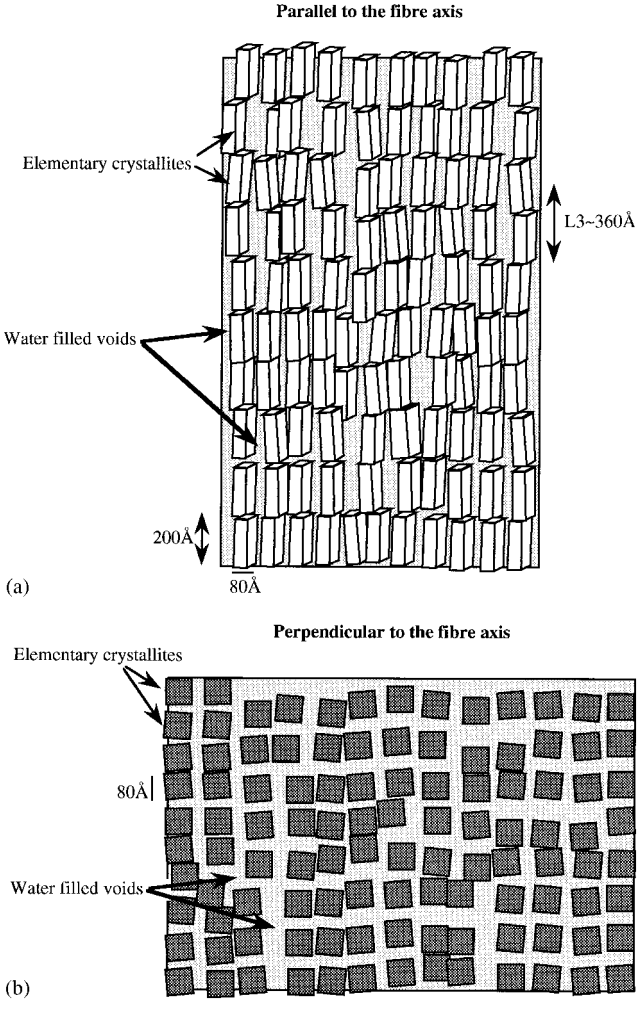

Fig. 4. Schematic diagram showing the microstructure of water-swollen Tencel fibres (a) parallel to the fibre axis and (b) perpendicular to the fibre axis. The crystallite dimensions proposed by Lenz and Schurz [1] are used together with the data from Table 1. For simplicity, the elementary fibrils have been drawn as strings of elementary crystallites without showing the shorter connecting regions.

Table 1 summarises the trends identified, from Fig. 2, in changes in the void cross-section size and shape parameters L_2, R_3, S_3, X, Y, B_ϕ, L_3 and the implied changes in the volume fraction of the voids as the water-swollen untreated Tencel fibres were dried. These changes were typical of the changes observed in all of the fibres studied, at various stages of treatment, on dehydration.

3.1.2. Representation of void shape

From the estimated values for X, Y and L_3, it is clear that the voids in dry Tencel fibres are larger in all dimensions than those in wet Tencel fibres. Further, in water swollen and dry fibres the relative values of X, Y and L_3 suggest that the voids are long, thin ribbon-like structures as illustrated schematically in Fig. 3.

A rectangular void cross-section shape was assumed to obtain X and Y. If an ellipse is assumed, an anisotropic void cross-section shape of similar aspect ratio is found and similar changes are seen on drying.

3.1.3. Interpretation of the changes in cellulose microstructure on drying

Fig. 4 is a schematic illustration of the microstructure of water-swollen Tencel fibres. It uses the model for the microstructure of a lyocell type of fibre proposed by Lenz and Schurz. Elementary crystallites 200 Å long and 80 Å square in cross-section are assumed [1] in conjunction with the void dimensions, orientation and high volume fraction in Table 1. For simplicity, the elementary fibrils are drawn as strings of elementary crystallites without showing the shorter amorphous regions. It is likely that, in the wet fibres, there is an extensive network of small voids separated by either individual elementary fibrils or small groups of elementary fibrils. The idea of voids between groups of elementary fibrils is consistent with the concept of non-swelling clusters [3].

On drying, the void fraction falls and the void size rises, suggesting that a large number of voids close. It is possible that only the largest voids remain open in dried fibres. It is also possible that most voids collapse on drying, except a few, which are enlarged, perhaps by many small voids joining up. Fig. 5 is a schematic illustration of the microstructure of dry Tencel fibres.

3.2. Changing the pore structure with heat treatment

3.2.1. Observations

To reduce statistical uncertainty in the data, several 60 s frames of data from wet and dry samples were averaged, and error bars calculated. In all cases, the integrated equatorial intensity was extrapolated at low q using the Guinier method. High q extrapolation was only performed on the wet fibre data.

L_2, R_3 and S_3 for wet and dry fibres remained unchanged by treatment within the uncertainty of the experiment for both the untreated and pre-treated fibres. This indicates that the treatments did not affect the average void cross-section

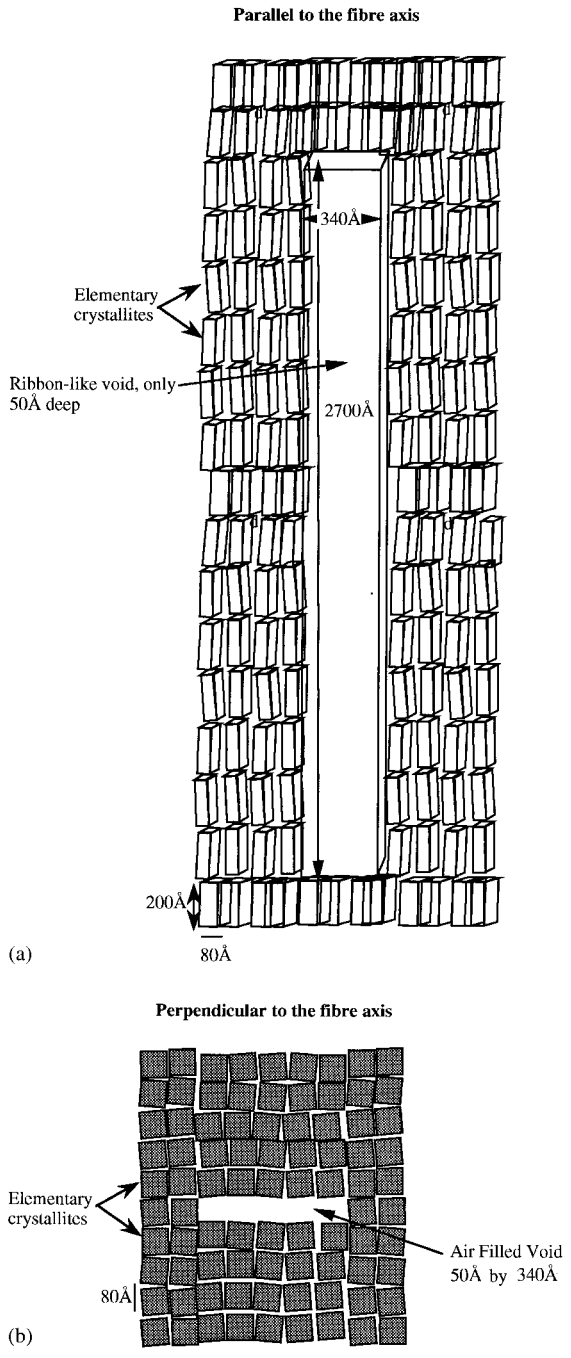

Fig. 5. Schematic diagram showing the microstructure of dried Tencel fibres (a) parallel to the fibre axis and (b) perpendicular to the fibre axis. The crystallite dimensions proposed by Lenz and Schurz [1] are used together with the data from Table 1. For simplicity, the elementary fibrils have been drawn as strings of elementary crystallites without showing the shorter connecting regions.

size in either the wet or dry fibre. Fig. 6(a) and (b) shows the scattering power divided by the appropriate density difference, Q/ρ^2, against treatment cycle for wet and dry, previously untreated fibres. Fig. 6(c) and (d) shows a similar set of plots for the in situ treatment of pre-treated Tencel fibres.

Azimuthal scan data were only available for the previously untreated Tencel fibres. During the four consecutive in situ soakings and dryings, B_ϕ remained approximately constant at $B_\phi \cong 20°$ for wet fibres and $B_\phi \cong 10°$ for dry fibres. From Fig. 7(a) and (b) it can be seen that L_3 for wet and dry fibres decreased with the increasing cycle number.

Fig. 6(a) shows that wet, previously untreated Tencel fibres showed a steady decrease in the volume fraction of voids after the first, second and third dryings at 160°C. The overall decrease in the volume fraction of voids in wet, previously untreated Tencel fibres was large. This decrease in volume fraction was accompanied by a decrease in the void length L_3, shown in Fig. 7(a).

The pre-treated wet fibre sample showed an overall decrease in the volume fraction of voids after successive dryings (Fig. 6(c)), but none quite so large as that seen for previously untreated Tencel fibres. This difference may be because the pre-treated Tencel fibres were less susceptible to further microstructural change, having already been modified in some way.

Dry, previously untreated Tencel fibres showed a steady increase in the void volume fraction after the first, second and third dryings (Fig. 6(b)). The overall increase in the volume fraction of voids in dry, previously untreated Tencel fibres was not as large as the decrease seen in wet fibres. This increase in volume fraction was accompanied by a decrease in the void length L_3, shown in Fig. 7(b).

Dry pre-treated fibres showed no convincing trends for any of the measured parameters as the number of cycles increased.

3.2.2. Interpretation of the changes in cellulose microstructure after successive wetting and drying cycles of Tencel fibres

In wet, previously untreated Tencel fibres, a reduction in the void volume fraction was accompanied by a decrease in the void length, L_3, parallel to the fibre axis with successive cycles. There was no significant change in the void dimensions perpendicular to the fibre axis. This is consistent with the hornification mechanism proposed for native cellulose [8]. During successive dryings, elementary fibrils surrounding voids are 'zipped up' by the formation of hydrogen bonds. On re-wetting, the structure cannot swell to the same extent. Voids may be either partially, or totally 'zipped up'; partial 'zipping up' would account for the reduction in void length. The fall in average void volume with successive cycles, implied by the fall in L_3, is not enough to account for the fall in volume fraction of voids implied by the changes in Q/ρ^2. This suggests that many voids are completely 'zipped up' on drying.

The smaller changes in the void volume fraction and length observed in water-swollen Tencel fibres after successive drying cycles and after pre-treatment compared with those for previously untreated Tencel fibres are consistent with the possibility that some voids are 'zipped up' by drying. Fig. 8 is a schematic illustration of changes that occur in the void population of water-swollen Tencel fibres during repeated swelling and drying cycles.

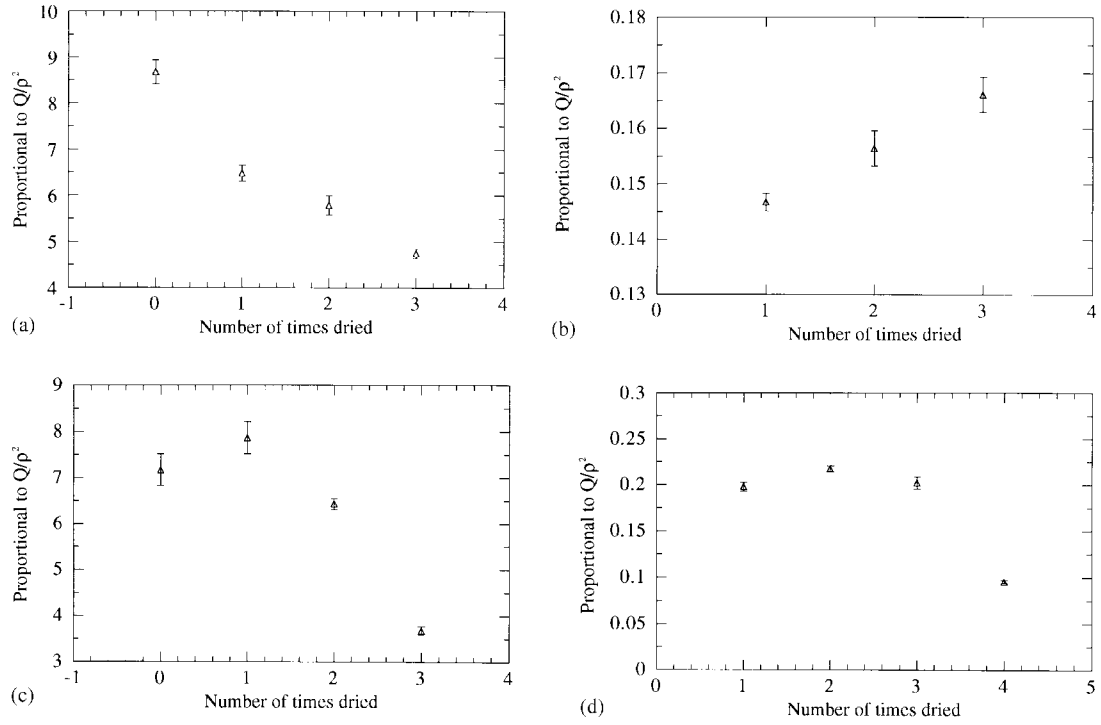

Fig. 6. The scattering power of Tencel fibres, divided by the electron density difference between cellulose and void, Q/ρ^2, for: (a) previously untreated water-swollen Tencel fibres, dried at 160°C and re-swollen four times, and observed wet; (b) previously untreated Tencel fibres swollen and dried three times, and observed dry; (c) pre-treated water swollen Tencel fibres, dried and re-swollen four times, and observed wet; and (d) pre-treated Tencel fibres swollen and dried three times, and observed dry.

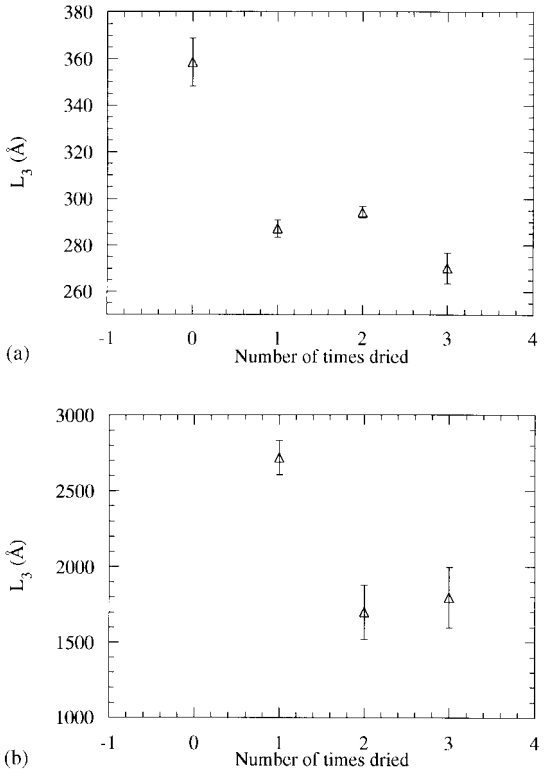

Fig. 7. L_3 of previously untreated Tencel fibres plotted as a function of drying cycle (a) dried and re-swollen four times, and observed wet and (b) swollen and dried three times, and observed dry.

In dry, previously untreated Tencel fibres, the void volume fraction increased after successive dryings at 160°C. This was accompanied by a decrease in L_3 and by no significant change in L_2, R_3 and S_3. Again it may be that the elementary fibrils surrounding a void have become 'zipped up' along part, or all, of the void length, giving rise to voids that are shorter in the dimension L_3. The rise in void volume fraction in the dry fibres may be due to the fibre structure being able to accommodate more short voids than the original longer voids. It is feasible that changes in the bonding between elementary fibrils might result in a change in the distribution of voids, perhaps creating two short voids in the place of one long one.

It appears that the hornification, with its associated increase in bonding between elementary fibrils, occurs in Tencel fibres during the treatments applied. Since bonding between fibrils is thought to affect fibrillation [5], it would be of interest to compare the extent of fibrillation of Tencel fibres before and after drying and re-swelling treatments.

4. Conclusions

Wet fibres have an extensive network of small voids. On dehydration these voids close up leaving larger voids, but a much lower overall volume fraction of voids. On re-wetting the volume fraction and the average length of the voids along the fibre direction is smaller than that for the original

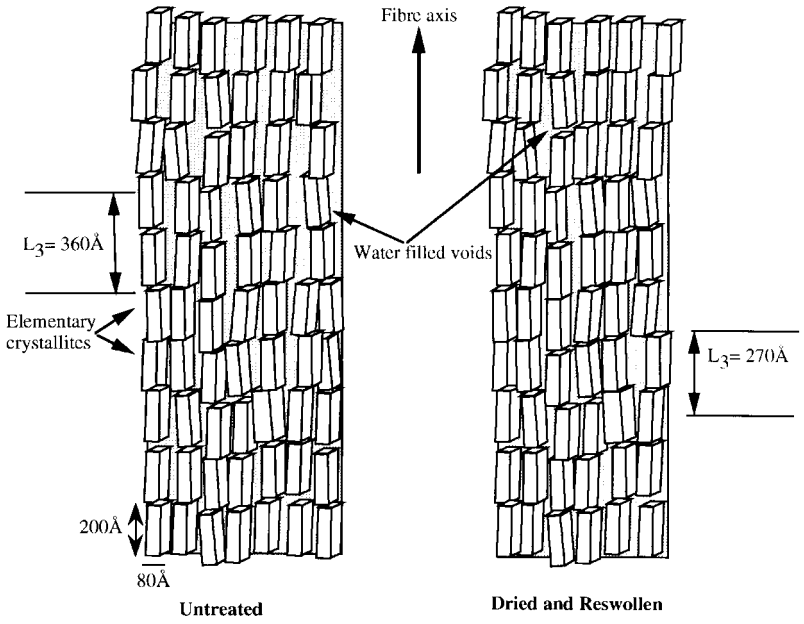

Fig. 8. A schematic illustration of the possible changes in the wet microstructure of Tencel fibres subjected to several swelling–drying cycles. The treatment causes some voids to 'zip up' to give a smaller length along the fibre axis, but a largely unchanged cross-section perpendicular to the fibre axis. Some voids are completely zipped up, contributing to the lower void volume fraction.

wet fibre. Successive drying and re-wetting leads to still shorter voids and lower volume fractions. The implication is that during void closure on drying, the hydrogen bonding between elementary fibrils increases and the structure does not open again to the same extent on re-wetting, in a response analogous to hornification in native cellulose. These changes in bonding may well affect the susceptibility of the fibres to fibrillation.

Acknowledgements

The authors are grateful to Courtaulds Corporate Technology (now part of the Akzo Nobel group) for samples and financial support, and to the EPSRC for funding. The X-ray experiments were performed on station 2.1 at the CLRC Daresbury laboratory with the help and advice of Drs S. Slawson and A. Gleeson. Thanks are due to Miss C.E. Moss for assistance with the analysis. Tencel® is a registered trademark of Akzo Nobel.

References

[1] Lenz J, Schurz J. Macromolecular Symposia 1994;83:273.
[2] Lenz J, Schurz J, Wrentschur E. Die Angewandte Makromolekulare Chemie 1995;229:175.
[3] Lenz J, Wrentschur E. J Appl Polym Sci 1988;35:1987.
[4] Kratky O, Miholic G. J Polym Sci, Part C 1963;2:449.
[5] Lenz J, Schurz J, Wrentschur E. J Colloid Polym Sci 1993;271:460.
[6] Mieck KP, Langner H. Studies on the tendency to fibrillate of man-made cellulose fibres produced by different fibre forming mechanisms (informal document, no date).
[7] Stone JE, Scallan AM. Technical section of the British Paper and Board Makers' Association, 1996, p. 1.
[8] Laivins GV, Scallan AM. Transcript of products of paper making. In: Baker CF, editor. Tenth Fundamental Research Symposium, 2. Oxford: Pira International, 1993. p. 1235.
[9] Scallan AM. Fibre–water interactions in paper making. 1. Transactions of BPBIF Symposium, Oxford, 1977.
[10] Stone JE, Scallan AM. Technical Section of The British Paper and Board Makers' Association, 1966, p. 1.
[11] Statton WO. J Polym Sci 1956;22:385.
[12] Statton WO. J Polym Sci 1962;58:205.
[13] Ruland W. J Polym Sci, Part C 1969;28:143.
[14] Wang W, Ruland W, Cohen Y. Acta Polym 1993;44:273.
[15] Shioya M, Takaku A. J Appl Phys 1985;58:11.
[16] Glatter O. In: Glatter O, Kratky K, editors. Small angle X-ray scattering, New York: Academic Press, 1982 chap. 4.
[17] Porod G. In: Glatter O, Kratky O, editors. Small angle X-ray scattering, New York: Academic Press, 1982 chap. 2.
[18] Crawshaw J, Vickers ME, Briggs N, Heenan RK, Cameron RE. Polymer 2000; in press.
[19] Langford JI. J Appl Crystallogr 1982;11:10.